

X-811-74-170

PREPRINT

NASA TM X- 70737

**VARIABLE BEAMWIDTH MONOPULSE FEED
FOR
TRACKING AND DATA RELAY SATELLITE
(TDRS)**

R. F. SCHMIDT

JUNE 1974



**GODDARD SPACE FLIGHT CENTER
GREENBELT, MARYLAND**

(NASA-TM-X-70737) VARIABLE BEAMWIDTH
MONOPULSE FEED FOR TRACKING AND DATA
RELAY SATELLITE (TDRS) (NASA) 30 p HC
\$4.50

CSCI 17B

N74-31611

G3/07

Unclas
47316

VARIABLE BEAMWIDTH MONOPULSE FEED
FOR
TRACKING AND DATA RELAY SATELLITE
(TDRS)

R. F. Schmidt

June 1974

GODDARD SPACE FLIGHT CENTER
Greenbelt, Maryland

VARIABLE BEAMWIDTH MONOPULSE FEED FOR TDRS

R. F. Schmidt

Network Engineering Division

ABSTRACT

This document discusses a means of providing the Tracking and Data Relay Satellite (TDRS) with a set of circularly-polarized, amplitude-sensing monopulse patterns suitable for acquiring and tracking user spacecraft at Ku-band (15.0 GHz). The possibility of increasing the less than 0.4-degree half-power beamwidth of the data beam to almost 1.0 degree during the acquisition phase is predicated on the use of feeds situated in the first bright-ring of the Airy diffraction structure. A complex-vector simulation equivalent to the Kirchhoff-Kottler or Franz formulations is used to compute transmitted and received field information for a dual-reflector (Cassegrain) antenna configuration in a three-dimensional space.

CONTENTS

| | <u>Page</u> |
|---|-------------|
| ABSTRACT | iii |
| INTRODUCTION | 1 |
| GEOMETRY | 2 |
| MONOPULSE DATA BEAMS | 3 |
| MONOPULSE ACQUISITION BEAMS | 3 |
| SUMMARY | 5 |
| ACKNOWLEDGMENTS | 5 |
| REFERENCES | 6 |
| APPENDIX A. ACQUISITION | A-1 |
| APPENDIX B. LINK MARGIN | B-1 |
| APPENDIX C. GEOMETRICAL PARAMETERS | C-1 |
| APPENDIX D. FEED CALCULATIONS | D-1 |
| APPENDIX E. ACQUISITION BEAM CALCULATIONS | E-1 |

ILLUSTRATIONS

| <u>Figure</u> | <u>Page</u> |
|---|-------------|
| 1 Sum pattern ($i = 1 \rightarrow 4$) ¹ | .7 |
| 2 Difference pattern ($i = 1 \rightarrow 4$) | .8 |
| 3 Sum pattern ($i = 5 \rightarrow 12$) | .9 |
| 4 Difference pattern ($i = 5 \rightarrow 12$). | .10 |
| 5 Sum pattern ($i = 1 \rightarrow 12$) | .11 |
| A-1 Surface error (inches rms) vs. antenna diameter | .A-1 |
| A-2 Antenna size vs. gain | .A-3 |
| A-3 Antenna size vs. gain and pointing accuracy, 14 GHz | .A-5 |
| B-1 User EIRP vs. tracking accuracy and data rate | .B-2 |
| C-1 Cassegrain geometry | .C-2 |
| C-2 Feed disposition | .C-3 |
| E-1 Circuitry for acquisition (Σ) beam | .E-3 |

Tables

| <u>Table</u> | <u>Page</u> |
|---|-------------|
| A-1 Antenna pointing error budget | .A-4 |

¹The letter (i) is used as a subscript for the feeds.

VARIABLE BEAMWIDTH MONOPULSE FEED FOR TDRS

INTRODUCTION

The Tracking and Data Relay Satellite (TDRS) Ku-band antenna has a nominal diameter of 12.5 feet (3.8 meters) which, at 15.0 GHz, implies a half-power beamwidth of approximately 0.4 degree. Even when ephemeris data on a user spacecraft are available, the narrowness of the Ku-band data beam will necessitate a mechanical (gimballed) search routine lasting 1 minute. Fuel consumption is required to compensate for spacecraft attitude errors resulting from the antenna motion. This technological problem was verified by both Rockwell, Inc. and Hughes Aircraft Company in the process of their definition phase study contracts for the TDRS completed in 1973¹.

This document discusses a means of providing the TDRS with a set of circularly-polarized, Ku-band, amplitude-sensing monopulse sum and difference patterns suitable for acquiring user spacecraft without incurring the penalties named above. A beamwidth increase of 150 percent ($BW_{acq} = 2.5 BW_{data}$) for the sum channel, with a proportionate reduction of the slope of the error channel, was observed using a Kirchhoff vector simulation. The magnitude of beamwidth broadening obtained would greatly alleviate the acquisition problem, but it remained to demonstrate that link gain had not been degraded excessively and that the approach was physically realizable². Simultaneous Ku-band and S-band operation is required for the spacecraft, the latter being obtained by means of a dichroic hyperboloid and focal-point feed (See Fig. C-1).

A simple means of attaining a variable beamwidth (zoom) capability, generally, is to avoid analogue techniques and settle for a discrete or quantized approach. It is sufficient in many cases, including the present TDRS problem, to switch electrically between a wide beam and a narrow beam state only. In this way, it is also possible to avoid the mechanical displacement of antenna elements on the spacecraft and attendant practical difficulties. Because a circular polarization capability was associated with the TDRS monopulse antenna, polarization techniques such as twist reflectors or gratings were specifically ruled out as a means of increasing antenna beamwidth.

According to a TDRS link analysis, the acquisition function can be degraded as much as 20 decibels, with reference to the high-gain data beam, and utilization of the first Airy bright-ring of the diffraction structure becomes a candidate technique³. It is noted that a desired 150-percent beamwidth increase, for

¹Appendix A.

²Background on the subject of variable beamwidth techniques can be found in Ref. 1.

³Appendix B

nearly circularly symmetric beams with ordinary sidelobe structure, implies a reduction of directivity gain in the amount of nearly 8 decibels. This follows from

$$G = \eta \left(\frac{\pi D}{\lambda} \right)^2 = \eta \left(\frac{\pi D_0}{\lambda} \right)^2 \left(\frac{1}{6.25} \right)$$

where D is a generic diameter and D_0 is the effective antenna diameter prior to beam widening. It is also noted that the ratio of power received in the Airy bright-disc to that of the first bright-ring region is about 19 to 1, which implies a difference of approximately 12.8 decibels, and establishes a lower bound for link degradation if the bright-ring alone is utilized to develop the acquisition function. These figures are based on a focal-region mapping of the time-average Poynting vectors passing through the Airy disc and first bright-ring in the conjugate focal plane. (See also Appendix E.)

GEOMETRY

The Cassegrain geometry used to explore the possibilities of achieving a variable beamwidth antenna on the TDRS, together with the parameters actually used for the Kirchhoff simulation, are given in Appendix C¹. All Ku-band feeds are situated at the conjugate focus (F^*) of the system and the S-band feed is situated at the focus (F) of the paraboloid. Only the development of the Ku-band feed is discussed in the present document.

An intermediate near-field mapping of the focal region fields, in the conjugate focal plane, indicated that the radius of the Airy disc was 2.7λ and the radius of the first bright-ring extended to approximately 4.7λ . The results are reasonable for the geometry used here because the radius of the Airy disc can be approximated directly from

$$R_{ad} = R_0 M = \frac{1.22 FM\lambda}{D} = \frac{(1.22)(5.0)(5.5)\lambda}{12.5} = 2.68\lambda$$

where R_0 is the corresponding disc radius for a paraboloid. The magnification factor of the system is

$$M = \frac{\epsilon + 1}{\epsilon - 1} = 5.5$$

based on the hyperboloid eccentricity²

$$\epsilon = [1 + (a/c)^2]^{1/2} = [1 + (1.300/1.247)^2]^{1/2} = 1.445$$

¹Ref. 2.

²The equations used for the conics can be found in Appendix C.

From the preceding, a feed diameter of 2.0λ was chosen for each of four feeds in the Airy disc and eight feeds in the bright-ring. The disposition used is illustrated in Appendix C. A value of $N = 10.0$ [implying a directive gain $G = 2(2N + 1)$] was assigned in the illumination function for the electric field

$$\mathcal{F} = S \cos^N \theta$$

in accord with the 2.0λ circular apertures selected. Details can be found in Appendix D.

Although the diffraction simulation utilized 12 distinct feeds to achieve monopulse patterns for the wide beam and narrow beam states, multimoding techniques may be preferred¹. This would have the advantage of eliminating septa and combining circuitry, but at the expense of introducing the waveguides associated with a multimoding technique. It may also be possible to utilize four feeds in the Airy first-ring to obtain the same "capture" area provided by the eight feeds of the simulation. The state-of-the-art development for specialized feeds should be reviewed when this concept is reduced to practice.

MONOPULSE DATA BEAMS

The high-gain or "narrow-angle" set of monopulse patterns obtained by the simulation are given as Fig. 1 and Fig. 2. Four feeds were situated in the Airy disc of the conjugate focal plane, as described previously, to obtain these patterns. Both phase and amplitude data are presented. It is noted that the half-power beamwidth of the data beam is approximately 0.36 degree, and that the ambiguity region begins at $\theta = 0.45$ degree. Sidelobe levels somewhat better than 20 decibels are indicated. The crossover level of these patterns is approximately 4.5 decibels. These, and all succeeding patterns, were obtained on an IBM 360/91 in approximately 3 minutes using a polar sampling grid of 5-wavelength resolution on the paraboloid and 0.5-wavelength resolution on the hyperboloid.

MONOPULSE ACQUISITION BEAMS

A set of monopulse patterns was obtained by the simulation using eight feeds situated in the first Airy bright-ring (See Fig. 3 and Fig. 4). The sum pattern did not broaden, but was in fact narrower than the data beam, and had interferometer-like characteristics due to the widely separated feeds. Its beamwidth was 0.22 degree, or approximately half of the half-power beamwidth of the data beam, and the first sidelobe was equal to the on-axis intensity. The difference pattern exhibited excellent characteristics with respect to both amplitude and phase. A relaxed, monotonic error slope out to $\theta = 0.50$ degree was observed, and the phase variation with respect to the polar angle

¹Ref. 3, Ref. 4.

was approximately 10 electrical degrees out to $\theta = 0.75$ degree¹. This set of patterns was obtained for the same surface resolution used previously in the evaluation of the Kirchhoff integrals, and with comparable running times.

Because the sum pattern obtained by means of the ring feed was narrower instead of broader than the original data beam, an attempt was made to utilize the interferometric pattern of Fig. 3 in combination with the original data beam. Due to the disparity of energy contained in an Airy disc and first bright-ring, a direct combination of the patterns is ineffective. When a coupler is placed in the data beam line, however, the weak interferometric sum pattern is capable of "spoiling" or broadening the shape of the original data beam. Several parameters need to be selected at this point. The amount of decoupling and the relative phase of the two patterns being combined (in a ring hybrid here) must be determined. It was found that a data beam 5.6 decibels lower than that received by the four feeds in the Airy disc, corrected by 37 electrical degrees to form a "subtractive" or antiphase summation, led to a useful sum pattern for acquisition purposes.

Figure 5 shows the synthesized pattern obtained by the process described above. The resulting beamwidth is 0.95 degree, and should be compared to the original data pattern of 0.36 degree beamwidth. The phase variation with polar angle (θ) is constant out to $\theta = 0.62$ degree for the "wide-angle" error channel pattern. A sidelobe level of better than 15 decibels is observed for the "wide-angle" sum pattern. The pattern is almost monotonic over the tracking domain, exhibiting a weak (0.25 decibel) tendency toward bifurcation. It is concluded that the crossover level between the acquisition patterns is approximately 1.8 decibels, based on an axial gain degradation of 13.6 decibels.

Although the original four-element monopulse feed was retained when the acquisition feed was added, this may not be required. As noted earlier and discussed in Appendix B, the TDRS tracking requirement may be satisfied using the acquisition feeds only, permitting the use of a high efficiency, non-tracking data feed in the Airy disc.

Details of the calculations leading up to the formation of the acquisition sum pattern are included in Appendix E of this document. The results of Fig. 5 should not be regarded as "optimum" in any sense, even though both phase and coupling coefficient were varied in numerous combinations to further improve the shape of the pattern. It is suggested that only the form of the patterns, Fig. 1 through Fig. 5, be considered here. Comparison of pattern levels, particularly between the groups (Fig. 1 and 2, Fig. 3 and 4, and Fig. 5) can be misleading. For example, the patterns of the first two groups were obtained as "transmit" patterns using equal source strength for four and eight sources, respectively. A comparison of pattern levels for these two groups is best made by a "receive" argument based on the energy contained in the Airy disc and first bright-ring, as in Appendix E.

¹Ref. 5, p. 36.

SUMMARY

A Cassegrain system with a magnification factor of 5.5 was selected to simulate the TDRS Ku-band "narrow-angle" monopulse beams and develop a similar set of "wide-angle" beams for rapid acquisition of user spacecraft. An on-axis gain degradation of 18.1 decibels resulted from a technique which increased half-power beamwidth from 0.36 degree to 0.95 degree at 15.0 GHz. The approach used simply couples a fraction of the received power in the Airy disc and combines it with power contained in the first bright-ring of the focal region until acquisition is achieved. Depending upon the tracking accuracy requirements, (1) the acquisition feed will continue to provide autotrack of the user spacecraft while the non-tracking data beam provides forward and return link communication or (2) for greater tracking accuracy, the autotrack function would be switched from the acquisition feed to a tracking data feed.

The method of beam broadening described herein is predicated on the summation of certain radiation patterns. This is a critical aspect of the method. For example, it is not known at this time what the effects of selecting a different set of parameters for a Cassegrain configuration might be. A parallel effort is underway for a system with a magnification factor reduced from 5.5 to 2.0. The latter geometry is better suited to packaging in a nose cone shroud than the one explored in this document; however, TDRS antenna surface parameters have not been established at this writing. Near-field mappings of the focal region fields, wavefronts, and time-average Poynting vectors are being used extensively, together with the subsystem back-scattered patterns, to determine the mechanics of beam broadening when augmenting a system with a ring feed. This is an interim effort, and work is continuing on a variety of microwave zooming techniques.

ACKNOWLEDGMENTS

The author acknowledges inputs from the classical literature, periodicals, and journal papers. All computer programming and software tasks associated with this document were accomplished by R. Miezi and W. Bartley of Programming Methods, Inc. under contract to Goddard Space Flight Center. The basic concept of utilizing the Airy bright-ring to affect the width of the acquisition pattern is due to L. F. Deerkoski of the TDRSS Project Office. In addition, the author acknowledges technical discussions on the broad aspects of microwave zooming with M. Uyehara and J. Pullara of Martin Marietta Aerospace, as well as A. F. Durham and L. R. Dod of the Antenna Systems Branch, Network Engineering Division, Goddard Space Flight Center.

REFERENCES

1. Goddard Space Flight Center Document X-811-74-62.
2. Patent Disclosure NASA Case No. GSC-11,924-1.
3. Final Report for Low-Noise, High-Efficiency Cassegrain Antenna Studies, Hughes Aircraft Company, Contract No. NAS 5-3282.
4. Feasibility of Combined S- and X-band Feed for Reflector Antennas, Hughes Aircraft Company, Contract No. NAS 5-20111.
5. Rhodes, D. R., Introduction to Monopulse, McGraw - Hill Book Co, Inc., 1959.
6. Antenna Handbook, Washington Aluminum Company, Inc.

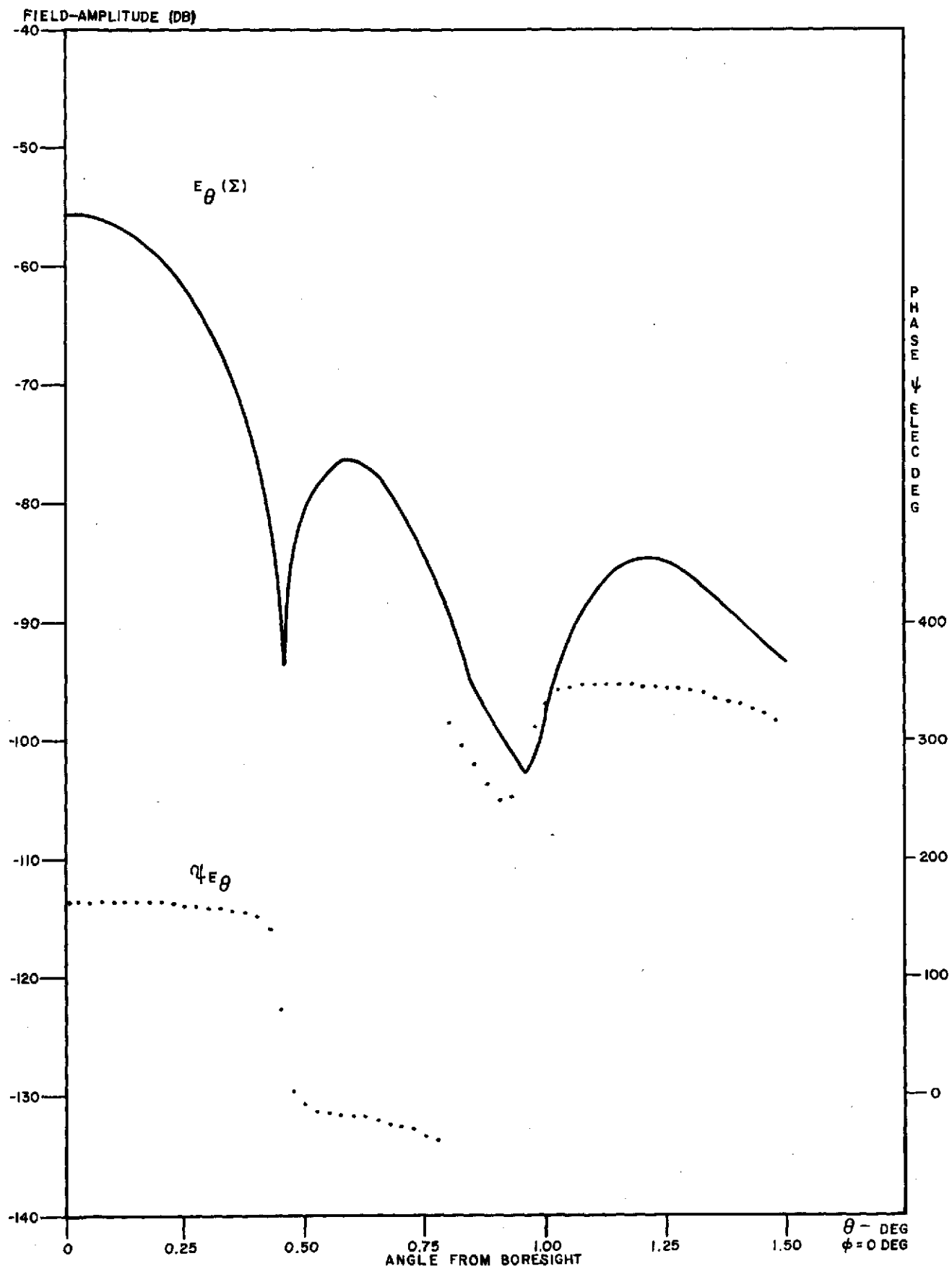


Figure 1. Sum-pattern ($i = 1 \sim 4$)

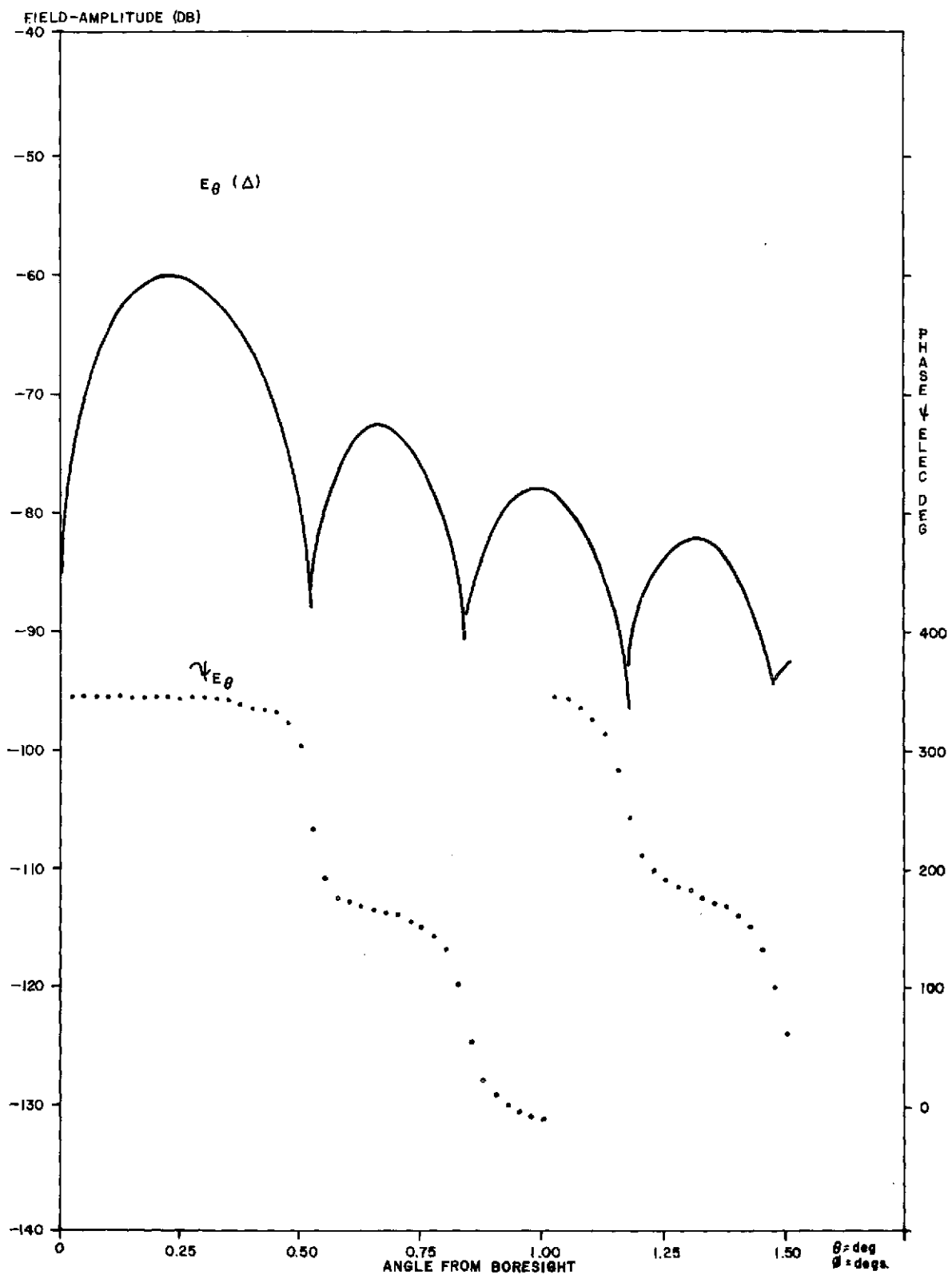


Figure 2. Difference-pattern ($i = 1 \rightarrow 4$)

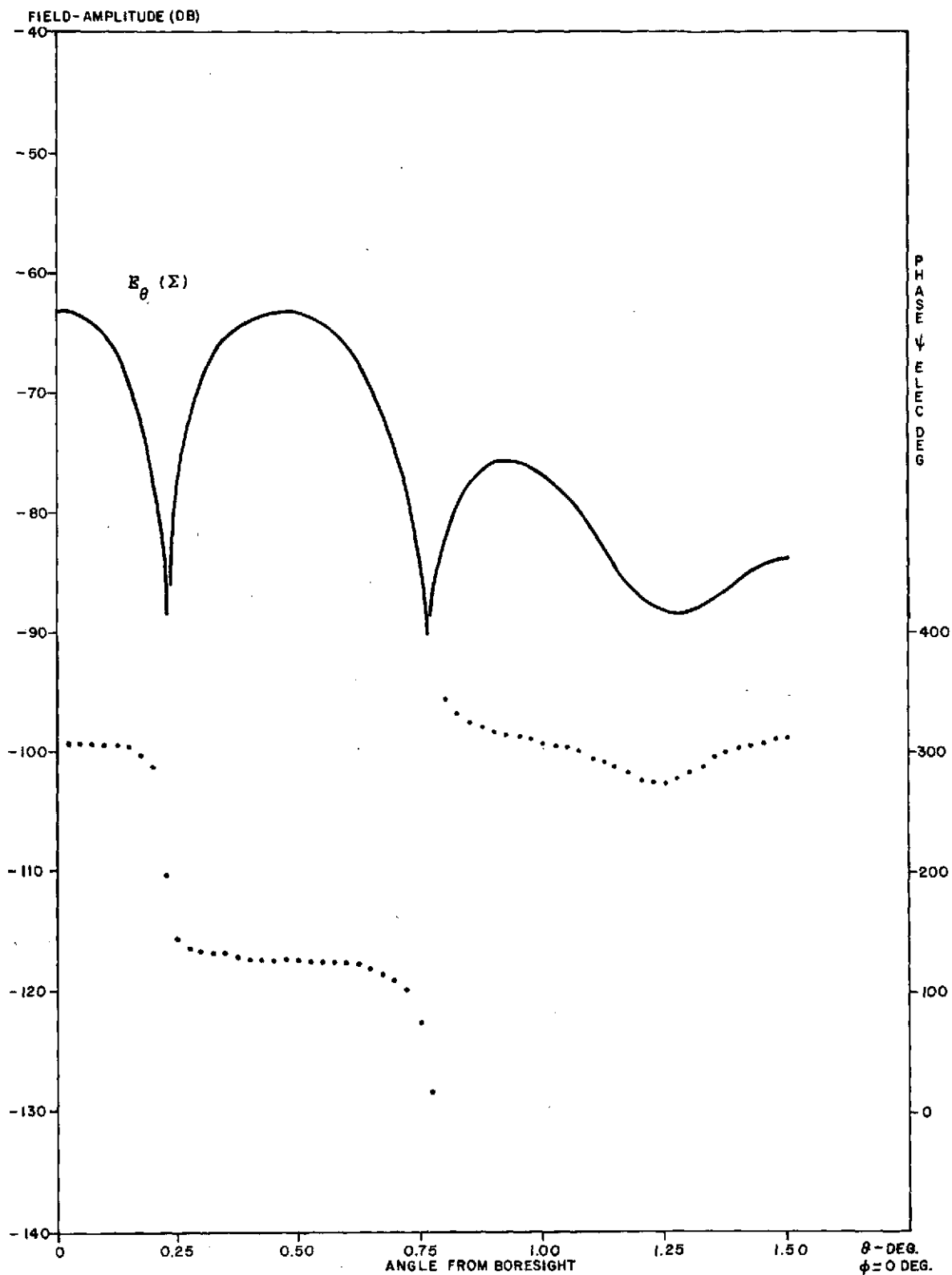


Figure 3. Sum-pattern ($i = 5 \rightarrow 12$)

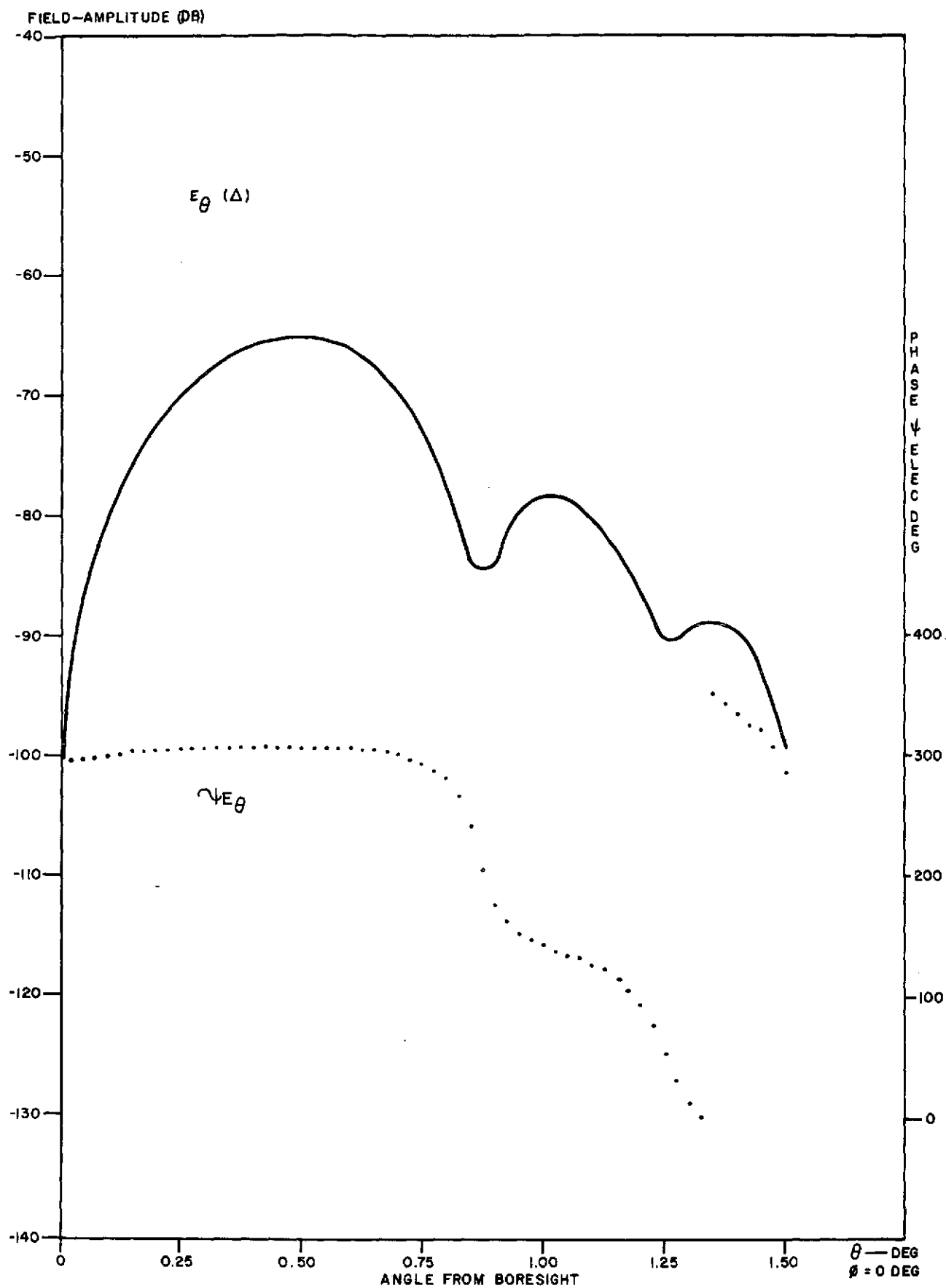


Figure 4. Difference-pattern ($i = 5 \rightarrow 12$)

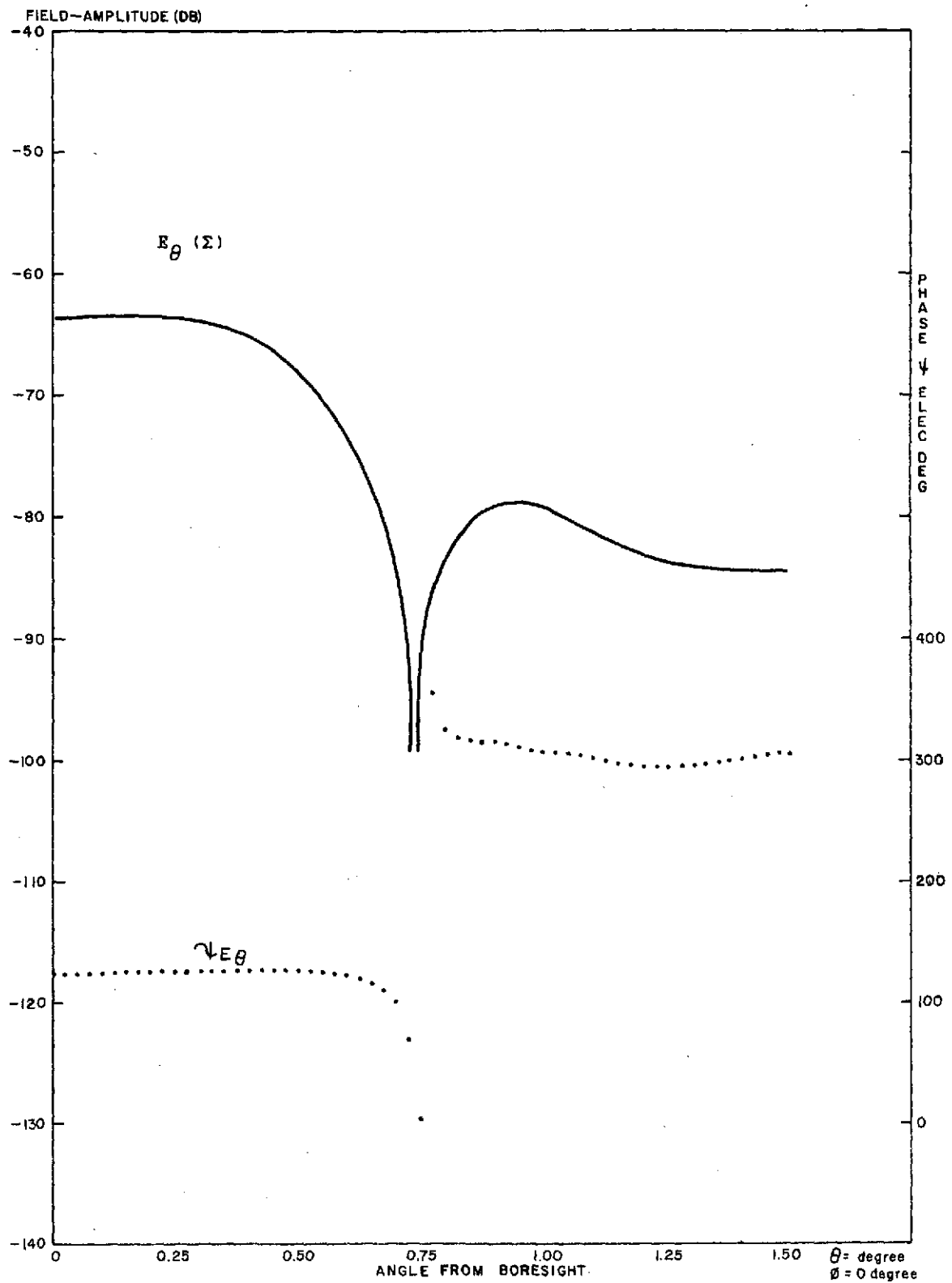


Figure 5. Sum-pattern ($i = 1 \rightarrow 12$)

APPENDIX A

ACQUISITION

The TDRS 12.5-foot antenna is capable of simultaneous operation at S- and Ku-bands for reception and transmission. To minimize user spacecraft impact, a 3.8-meter parabolic reflector was selected for SA service. Selection of this antenna was based on the surface tolerance of the reflector and the pointing capability of the TDRS. Figure A-1 indicates the three curves representing rms surface tolerance versus antenna diameter for deployable dual-mesh reflectors. The "design goal" curve was based on analysis and past experience with this technology, whereas the other two curves represent upper and lower bounds on the actual surface tolerance expected of the Advanced Applications Flight Experiments (AAFE) 3.8-meter antenna fabricated by Radiation, Inc. Experience indicates that there is a linear relationship between rms surface tolerance and antenna diameter for reflectors of 3.8 meters and larger.

Based on the upper and lower tolerance bounds (See Fig. A-1), the antenna gain can be plotted as a function of antenna diameter (See Fig. A-2). Depending on the actual σ/D , the antenna gain peaks between 30 and 50 feet diameter. The gain-versus-diameter curve becomes nonlinear at approximately 12.5 feet diameter. Increasing the diameter from 12.5 feet to 30 feet for a σ/D of 2×10^{-4} yields only a 2-dB gain increase as opposed to a theoretical increase of 7.5 dB that would result if surface tolerance were not significant.

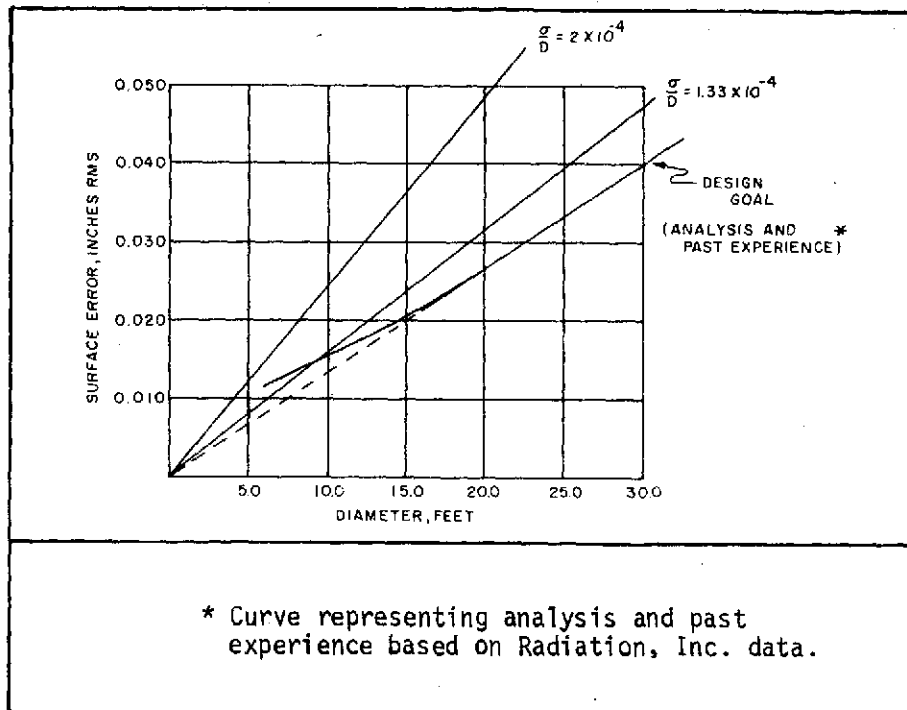


Figure A-1. Surface error σ (inches rms) vs. antenna diameter

The pointing capability of the TDRS is the second major criterion for SA antenna size selection. Table A-1 summarizes contributions to antenna pointing errors for initial operations. By autotracking Ku-band signals emitted by ground-based transmitters, time-invariant components to this error budget can be calibrated out, thereby improving the pointing capability of the antenna. Depending on the extent to which antenna system pointing uncertainties listed in table A-1 can be eliminated through calibration in orbit, the actual total pointing uncertainty in orbit will be between ± 0.3 and ± 0.5 degree. Figure A-3 indicates the pointing requirements (defined as 3-dB beamwidth/2) as a function of antenna diameter at Ku-band. Even at 12.5-foot diameter, the required pointing capability exceeds the ± 0.3 to ± 0.5 degree capability of the TDRS. The pointing requirement is a problem only during acquisition because an autotrack capability is included in the Ku-band feed. During acquisition the antenna must be commanded through a spiral scan routine to acquire the Ku-band signal of a desired user. This type of acquisition procedure is feasible and has been implemented in the past for similar requirements. It is desirable, however, to eliminate the mechanical scan procedure entirely by electronically broadening the Ku-band beam of the antenna for acquisition and returning to normal operation after autotracking is accomplished.

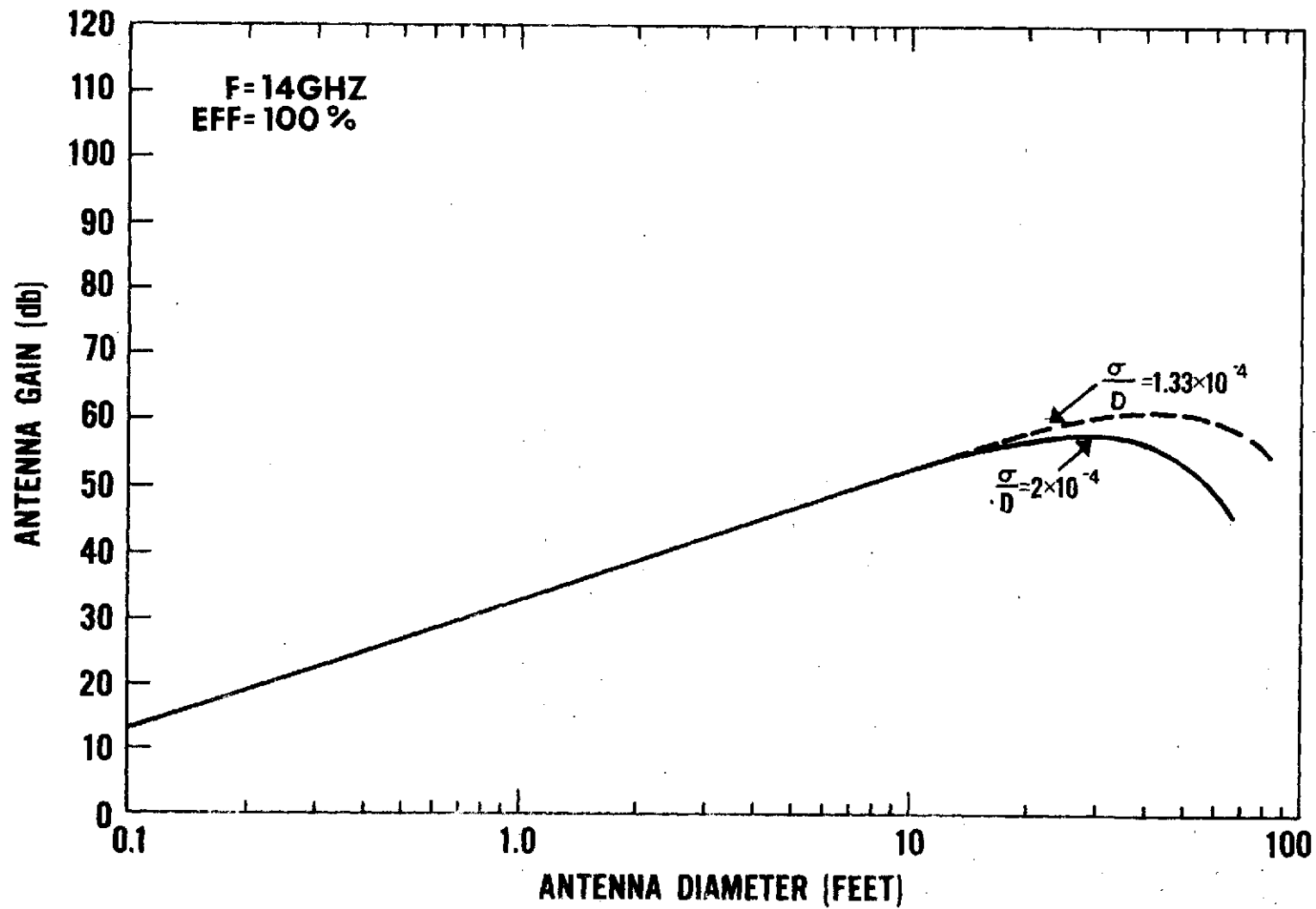


Figure A-2. Antenna size vs. gain

Table A-1. Antenna Pointing Error Budget¹

| | |
|--|--------------------|
| TDRS Attitude Uncertainties | |
| Sensor error | $\pm 0.1^{\circ}$ |
| Sensor alignment | $\pm 0.05^{\circ}$ |
| Nutation and control | $\pm 0.2^{\circ}$ |
| RSS total (each axis) | $\pm 0.23^{\circ}$ |
| RSS total (two axes) | $\pm 0.32^{\circ}$ |
| Antenna System Uncertainties | |
| Gimbal errors (two axes) | $\pm 0.14^{\circ}$ |
| Mechanical support mechanism for antenna and gimbal | $\pm 0.25^{\circ}$ |
| Misalignment between RF and mechanical axes of reflector | $\pm 0.05^{\circ}$ |
| RSS total (two axes) | $\pm 0.3^{\circ}$ |
| Total Pointing Uncertainty | $\pm 0.44^{\circ}$ |
| ¹ Reference <u>Part II Final Report, Tracking and Data Relay Satellite System Configuration & Tradeoff Study</u> , Space Division, Rockwell International, Contract No. NAS5-21705, dated April 1973. | |

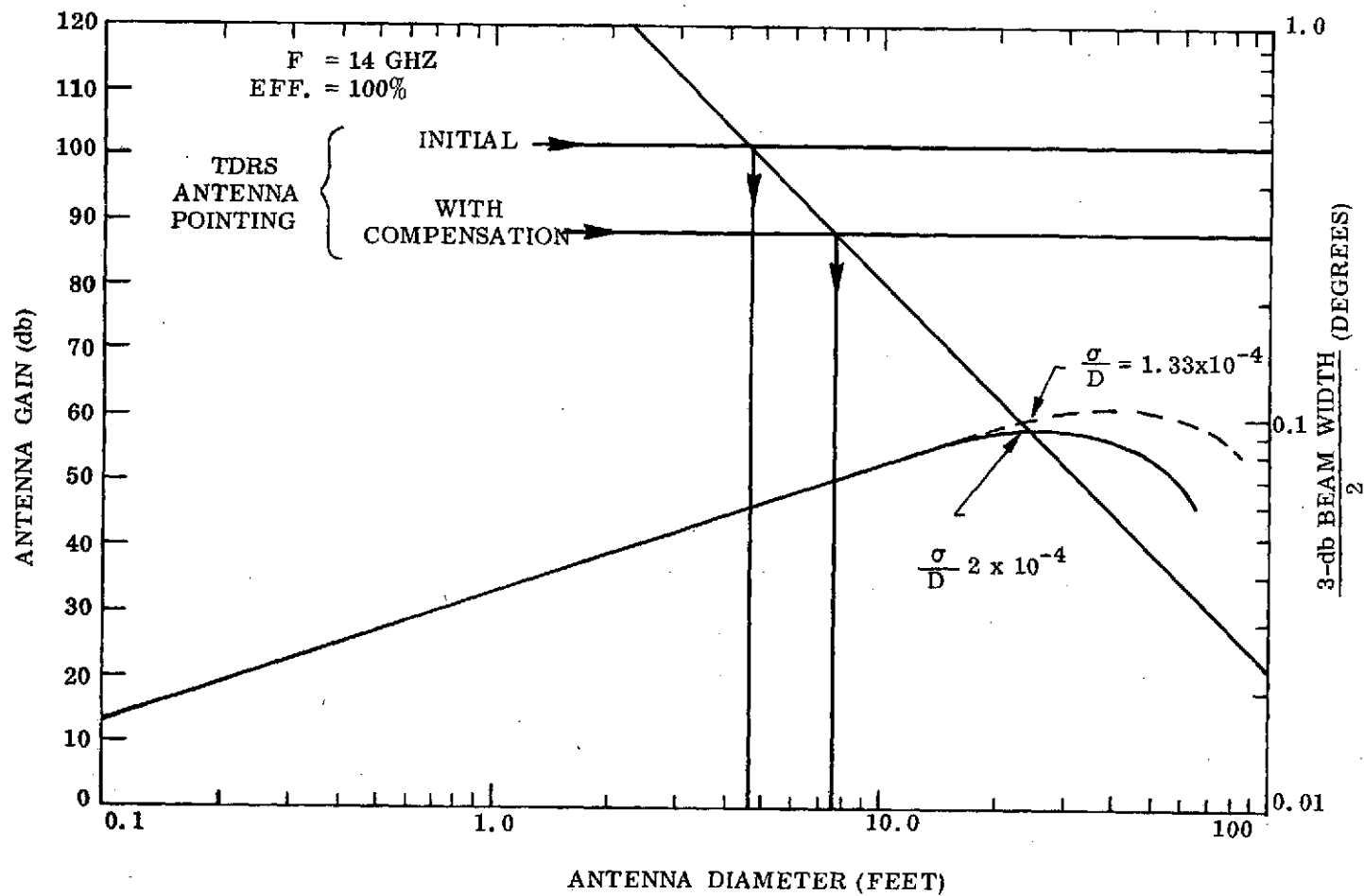


Figure A-3. Antenna size vs. gain and pointing accuracy, 14 GHz

APPENDIX B

LINK MARGIN

The autotrack accuracy of the TDRS antenna as a function of user spacecraft EIRP is shown in Fig. B-1¹. The minimum anticipated data rate at Ku-band is 1 Mb/s corresponding to an EIRP of 30 dBw. The TDRS requirement for autotrack is 0.07 degree rms. Therefore, approximately 20 dB of margin exists in the Ku-band return link relative to the tracking requirement.

The tracking accuracy plotted in Fig. B-1 is based upon near-boresight conditions where the error signals are small relative to the sum channel. For acquisition, the error channel signal levels will normally be 10-to-20 dB higher than those experienced under normal autotrack conditions and, therefore, the sum channel SNR becomes the important factor to consider rather than tracking accuracy. Assuming the 1-Mb/s user transmits an unmodulated carrier for acquisition, the 30-dBw EIRP represents a 20-dB SNR in the 1-MHz RF bandwidth required to encompass the worst case ± 450 kHz doppler. The TDRS antenna gain for acquisition can be decreased by up to 20 dB and still provide a positive SNR within the 1-MHz bandwidth.

¹Twelfth Monthly Progress Report, Contract NAS 5-20414, prepared by the Magnavox Company for the NASA/Goddard Space Flight Center, June 1974.

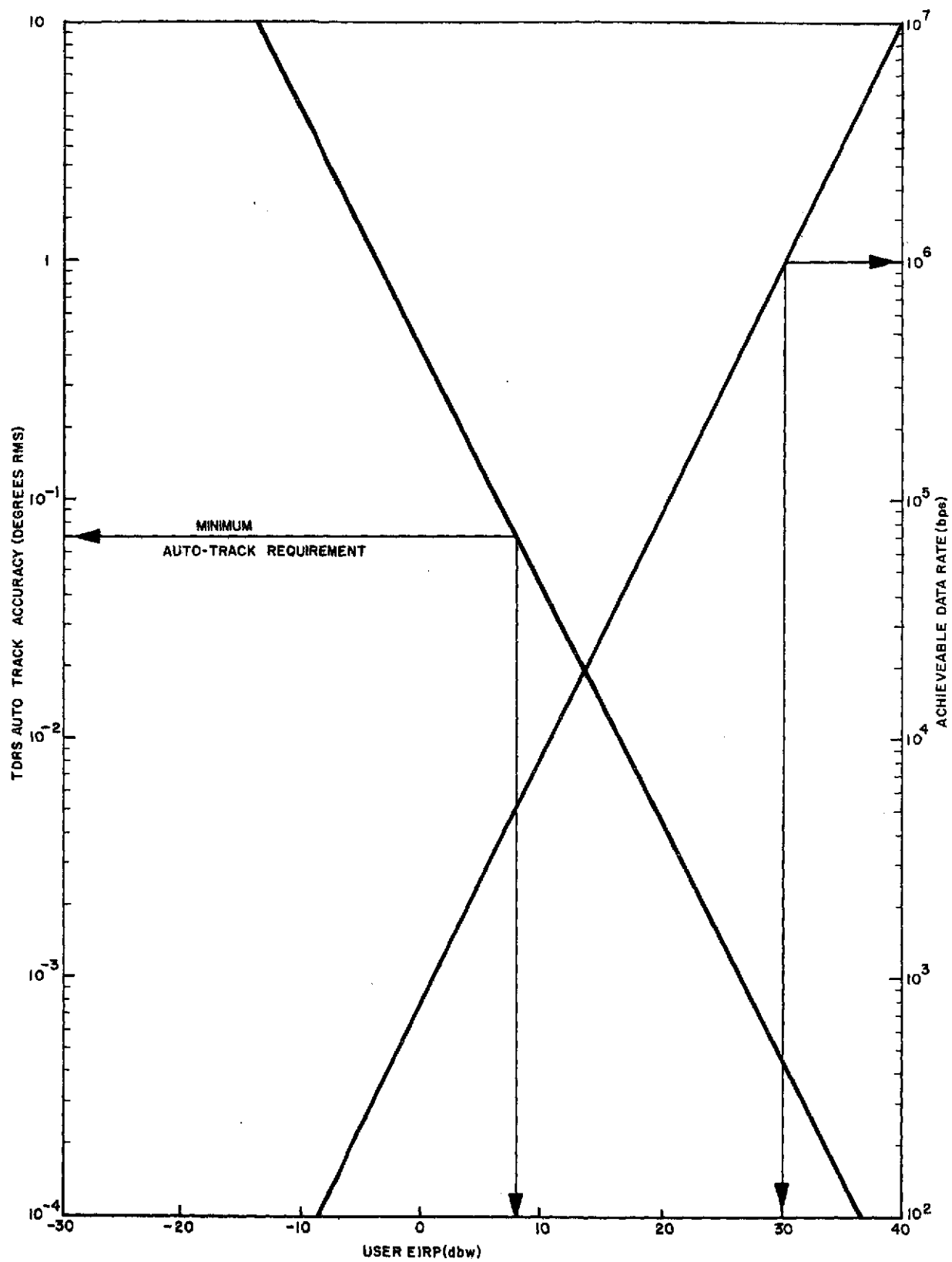


Figure B-1. User EIRP vs. tracking accuracy and data rate

APPENDIX C

GEOMETRICAL PARAMETERS

Paraboloid: $x = \sigma \sin \zeta, \quad y = -\sigma \cos \zeta, \quad z = \frac{\sigma^2}{4F} + z_{1p}$

$\sigma_o = 0.750' = \text{minimum radius}$

$\sigma_{\max} = 6.25' = \text{maximum radius}$

$F = 5.0' = \text{focal length}$

$z_{1p} = -F = \text{displacement}$

Hyperboloid: $x = \sigma \sin \zeta, \quad y = -\sigma \cos \zeta, \quad z = c (1 + \sigma^2/a^2)^{1/2} + z_{1h}$

$\sigma_o = 0.0' = \text{minimum radius}$

$\sigma_{\max} = 0.750' = \text{maximum radius}$

$a = 1.300' = \text{hyperboloid parameter}$

$c = 1.247' = \text{hyperboloid parameter}$

$z_{1h} = -c \epsilon = -1.802' = \text{displacement for confocal system}$

Note

σ and ζ are radial and azimuthal variables of a polar net.

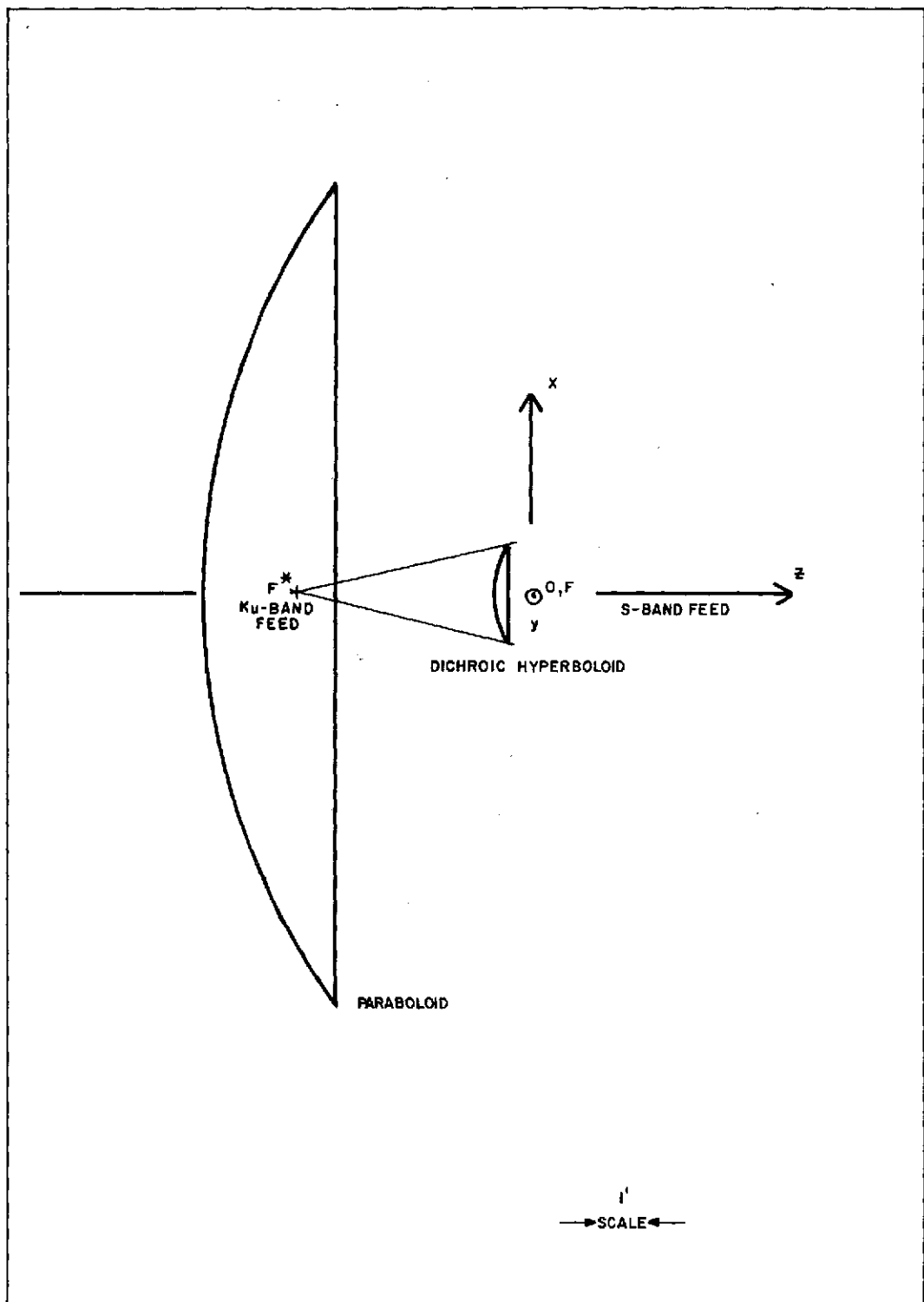
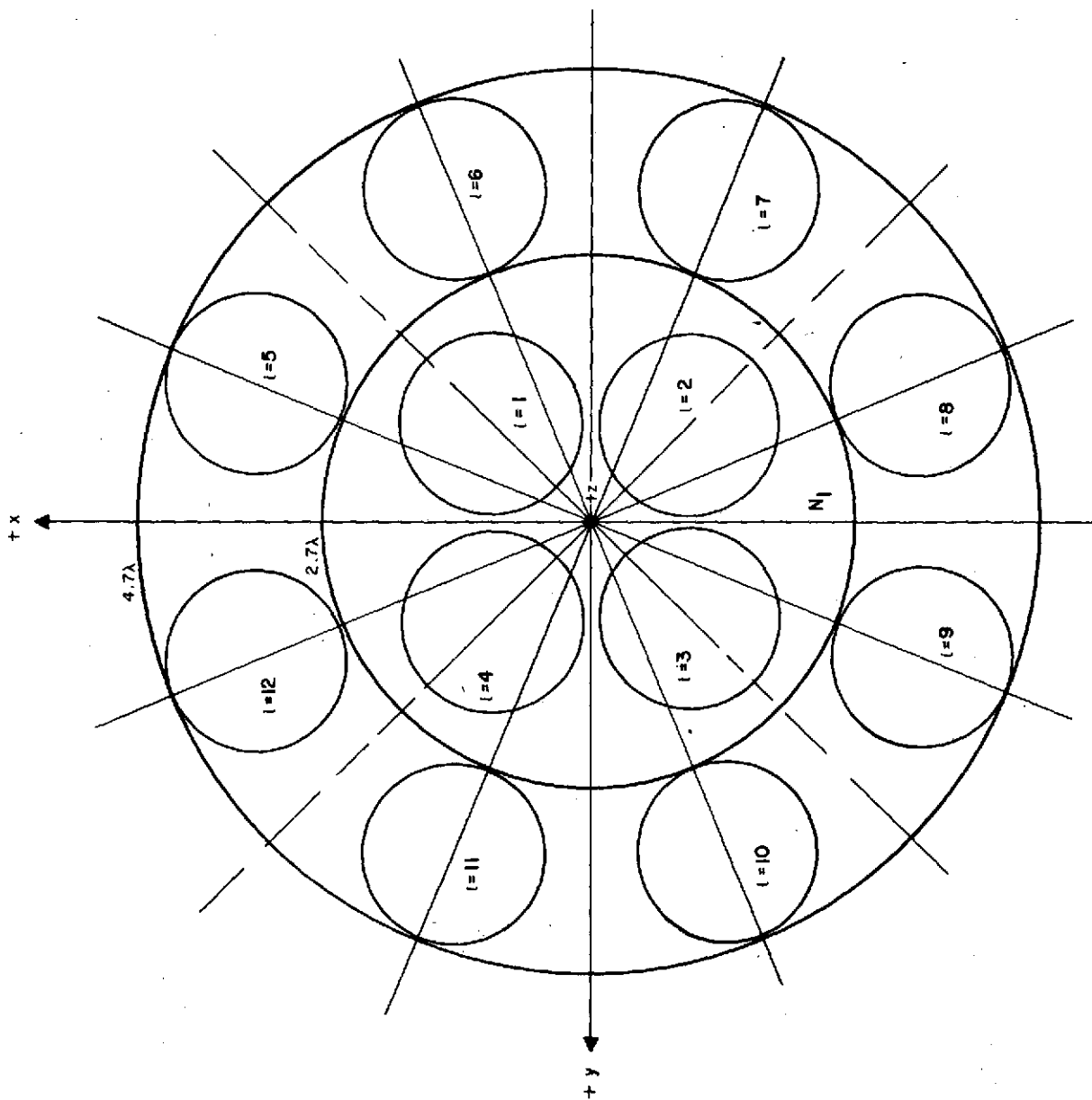


Figure C-1. Cassegrain Geometry



Note

N_1 and N_2 are the first and second nulls, respectively, of the diffraction structure in the conjugate focal plane (F^*). The region from axis Z to N_1 represents the Airy disc, and the annular region between N_1 and N_2 represents the first Airy bright-ring.

Figure C-2. Feed Disposition

APPENDIX D

FEED CALCULATIONS

One method of obtaining the value of N is to rely on handbook data¹ which relates aperture width to half-power beamwidth. The value $D = 2.0 \lambda$ implies $BW_{-3 \text{ dB}} = 2 \theta = 30^\circ$. From this it follows that

$$3 \text{ dB} = 20 \log_{10} \left(\frac{1}{\cos \theta} \right)^N$$

and the value $N = 10.0$ results.

A more fundamental approach is to apply the equation

$$G \approx \left(\frac{\pi D}{\lambda} \right)^2$$

which yields a directive gain value of $4\pi^2 \approx 40$. Since the feed function (\mathcal{F}) can be introduced into the definition of directive gain, and leads to the closed-form solution

$$G = 2(2N + 1)$$

for beams of one lobe, a value of $N \approx 9.5$ is obtained by equating the two expressions above.

¹Ref. 6, p. 5.

APPENDIX E

ACQUISITION BEAM CALCULATIONS

The ratio of the energies received by the Airy disc and first bright-ring, based on the integral of the power-density times (x) differential-area product, is

$$\frac{\iint_{\text{disc}} \bar{P}_d \cdot d\bar{s}}{\iint_{\text{ring}} \bar{P}_{r_1} \cdot d\bar{s}} \approx \frac{19}{1}$$

or 12.8 decibels. As noted previously, the "wide-angle" or acquisition sum pattern was obtained by superimposing a first pattern with the shape of the data beam and a second pattern having the shape of the interferometric or "spoiler" beam. The manner in which this was done can be set down in terms of electric fields as

$$\bar{E}_{\text{acq}}(\theta, \phi) = [C_1 \bar{E}_{\text{data}}(\theta, \phi) + \bar{E}_{r_1}(\theta, \phi) e^{-j\psi_0}] / \sqrt{2}$$

where the factor $\left(\frac{1}{\sqrt{2}}\right)$ anticipates summation in a ring hybrid, C_1 is a coupling factor, and ψ_0 is a phase delay required to effect a "subtractive" operation. A satisfactory beam (See Fig. 5) was obtained with a value of C_1 such that $10 \log_{10} \left(\frac{1}{C_1}\right)^2 = 5.6$ decibels, and $\psi_0 = 37$ electrical degrees.

Once the beam $\bar{E}_{\text{acq}}(\theta, \phi)$ has been formed there are several methods for determining its on-axis gain relative to the original data beam $\bar{E}_{\text{data}}(\theta, \phi)$. It is possible to proceed directly on the assumption that superposition, which satisfies Maxwell's linear equations, does not violate energy conservation even though power or energy are quadratic in the field quantities. It is also possible to use the rigorous definition of directive gain and evaluate

$$G = \frac{|\bar{E}_{\text{acq}}(\theta, \phi)|^2}{\frac{1}{4\pi} \int_0^{2\pi} \int_0^{\theta^2} |\bar{E}_{\text{acq}}(\theta, \phi)|^2 \sin \theta \, d\theta \, d\phi}$$

at $\theta = 0^\circ$, having developed the acquisition sum beam adequately in theta (θ) to make the integral meaningful. When $\theta = 5.0$ degrees, the pattern level is down 35 decibels from the axial value. This becomes a reasonable upper limit for theta because the Kirchhoff integration by which the antenna pattern is generated demands an ever-smaller resolution on the antenna surface for larger values of theta and, as a practical matter, the pattern must ultimately be truncated. The decoupling and directive gain losses then lead to an estimate of on-axis gain.

Finally, it is possible to proceed by a method which avoids energy paradoxes and does not make use of the pattern shape $E_{acq}(\theta, \phi)$ per se. It is sufficient that the energy ratio previously established for the Airy disc and first bright-ring is 12.8 decibels, and a first or "spoiler" beam intensity 7.2 decibels lower than a second or decoupled data beam constituted the inputs to a ring-hybrid for the on-axis condition. Since it has already been established that a phase correction (ψ_0) led to a "subtractive" rule of superposition, and because it is known that an ideal ring-hybrid conserves energy, the difference port of the hybrid will yield the on-axis value of the acquisition sum-channel beam. Figure E-1 illustrates the circuitry and all relevant signal levels at $\theta = 0^\circ$, the on-axis case. Since the acquisition sum-channel beam is -8.0 dB below the level of the decoupled data beam it follows that the former is -13.6 dB below the unmodified data beam level. The following is a comparison of the degradation estimates by the three methods described in this appendix:

| <u>Method</u> | <u>Degradation Estimates</u> |
|--------------------|-------------------------------------|
| Superposition | $\delta G \approx -13.4 \text{ dB}$ |
| Directive gain | $\delta G \approx -13.3 \text{ dB}$ |
| Airy disc and ring | $\delta G = -13.6 \text{ dB}$ |

None of the preceding computations include the significant spillover loss at the hyperboloidal subreflector. A spillover coefficient of $\eta_{so} = 0.35$ was obtained by numerical methods, which implies additional loss of 4.5 dB to the acquisition link. From this, it appears that the total degradation could be as high as $-13.6 \text{ dB} - 4.5 \text{ dB} = -18.1 \text{ dB}$.

E-3/E-4

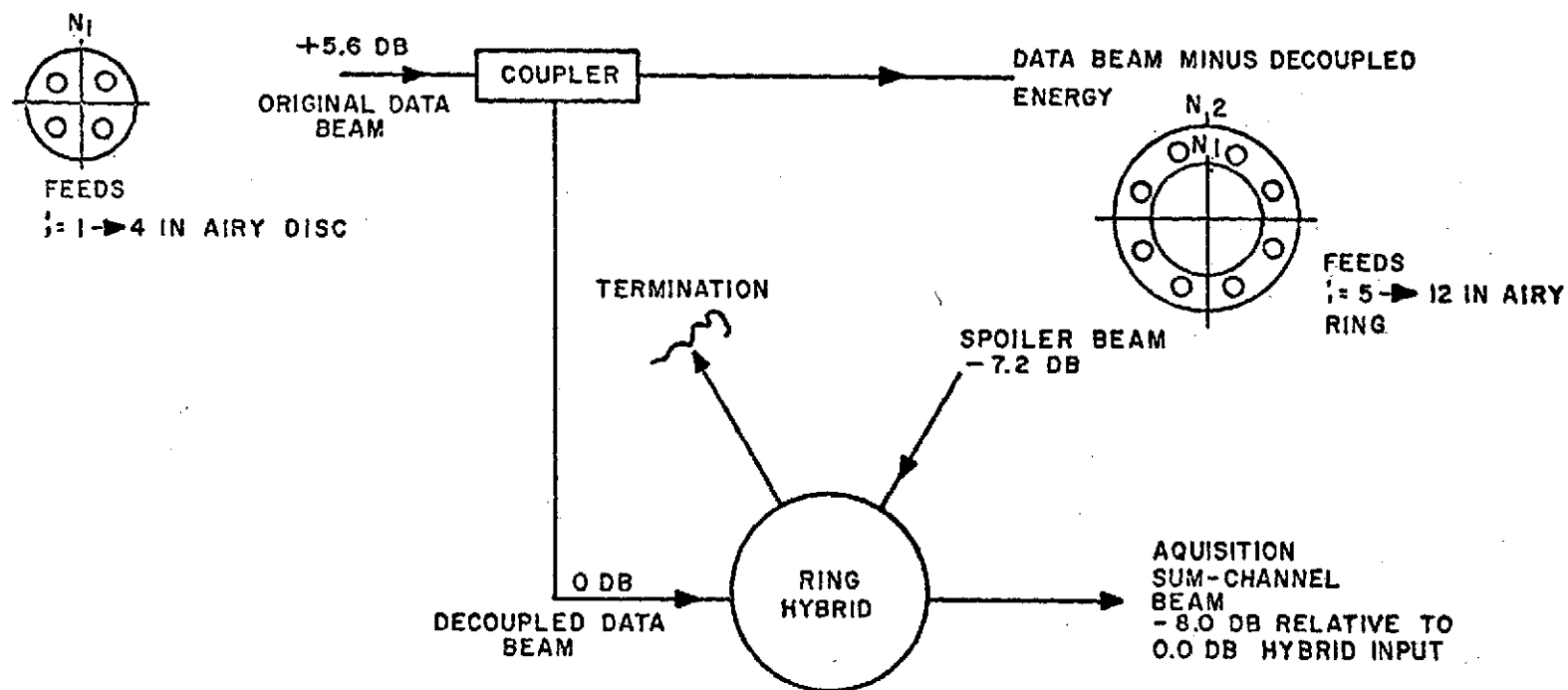


Figure E-1. Circuitry for acquisition (Σ) beam